IEEE Access
Multidisciplinary ⋮ Rapid Review ⋮ Open Access Journal

Received 15 May 2024, accepted 16 July 2024, date of publication 19 July 2024, date of current version 29 July 2024.

Digital Object Identifier 10.1109/ACCESS.2024.3431093

RESEARCH ARTICLE

Multi-Source Data-Driven Framework for Work State Classification in Fabric Pilling and Linting Performance Assessment

YUANQING MAO[1], QINGCHUN JIAO[2], ZIFAN QIAN[2], CHUNCONG WANG[3], AND TINGTING SUN[4]

[1]Zhejiang Market Regulation Digital Media Center, Hangzhou, China
[2]School of Automation and Electrical Engineering, Zhejiang University of Science and Technology, Hangzhou 310023, China
[3]Zhejiang Jinhui Digital Technology Company Ltd., Hangzhou, China
[4]Zhejiang Light Industrial Products Inspection and Research Institute, Hangzhou 310000, China

Corresponding author: Qingchun Jiao (jiaoqch@zust.edu.cn)

This work was supported in part by the National Science and Technology Plan Project of the State Administration for Market Regulation under Grant CY2023213, in part by the "Chu Ying" Core Project of Zhejiang Administration for Market Supervision under Grant 2022MK057, and in part by the Natural Science Foundation of Zhejiang Province under Grant LGG20F020008.

ABSTRACT Fabric pilling performance is one of the key indicators for evaluating textile quality, but there is limited research on the effectiveness of pilling detection traceability and non-intrusive monitoring of detection equipment operating status. In this paper, a multi-source data-driven method for classifying the working status of fabric pilling performance detection is proposed. This study constructs a real-time non-intrusive monitoring system for fabric pilling detection in a laboratory environment, collecting multiple types of data such as electrical parameters of pilling detection equipment, personnel behavior, and equipment noise. GoogLeNet convolutional neural network is used to recognize high-dimensional audio data and achieve feature dimension reduction. By constructing a multi-classification algorithm based on Decision Tree-Support Vector Machine (DT-SVM) for the pilling detection process, a minimum accuracy of 95.62% is achieved in practical operation. This system not only perceives the relevant influencing factors of detection activities without interfering with normal detection activities but also effectively distinguishes various detection working states, providing new ideas for the effectiveness traceability of pilling detection activities.

INDEX TERMS Non-intrusive monitoring, multi-source data-driven, fabric pilling performance, SVM multi-classification.

I. INTRODUCTION

As the primary raw material in textile production, fabrics play a crucial role in determining the quality and comfort of the final products [1]. With the improvement of living standards, consumers' demand for clothing has shifted from basic functionalities to a deeper pursuit of fabric quality and tactile sensation [2]. However, the common occurrence of fabric surface irregularities such as pilling and linting, resulting from friction between fibers leading to the formation of opaque particulate clusters, significantly impacts the visual appearance, tactile sensation, and durability of fabrics [3]. Complaints related to fabric pilling and linting account for as much as 29.51% of total textile quality issues [4], [5], underscoring the critical importance of fabric pilling and linting performance in assessing textile quality. Despite the crucial role of pilling and linting performance assessment in textile quality, there are still many challenges in current fabric pilling and linting detection, including susceptibility to factors such as equipment operation, personnel handling, and testing environments, as well as a lack of traceability of work states and non-intrusive diagnostics. Therefore, there is an urgent need for a comprehensive, accurate, and real-time non-intrusive monitoring system that integrates multi-source data analysis to effectively classify and trace the working states of fabric pilling and linting detection equipment.

The associate editor coordinating the review of this manuscript and approving it for publication was Xianzhi Wang.

Against this backdrop, this paper focuses on a research platform in a fabric testing laboratory, incorporating Non-Intrusive Monitoring (NIM) technology, aiming to maintain the original state of fabric pilling and linting detection, reduce subject bias, and enable real-time monitoring [6] The core of NIM technology lies in obtaining efficient and precise data for in-depth analysis and decision-making while minimizing interference with the tested objects [7] In this study, by adhering to the principles of NIM, we have developed a real-time non-intrusive monitoring system suitable for actual laboratory conditions and compliant with international standard testing requirements, enabling non-destructive monitoring of the entire fabric pilling and linting detection process. This paper introduces a workflow state classification methodology for fabric pilling performance inspection leveraging multi-source data. The principal contributions of this approach are summarized as follows:

(1) A comprehensive detection scheme for fabric pilling performance testing laboratories is proposed, which encompasses personnel activities, equipment power consumption, and instrument operating sounds throughout the inspection process. A real-time, non-intrusive monitoring system, tailored to the actual laboratory environment and conforming to standard testing requirements, has been designed. This system enables the sensing of diverse information related to inspection activities without interfering with routine testing procedures.

(2) In light of the varying noise levels inherent in different sensors during practical data acquisition, appropriate denoising techniques have been employed. To ensure temporal consistency among multiple data streams collected at disparate frequencies, sliding window approaches and interpolation techniques have been applied. Of note, audio data undergoes dimensionality reduction through Short-Time Fourier Transform (STFT), followed by feature extraction using the GoogLeNet model.

(3) A DT-SVM model has been established by integrating threshold classification with SVM classification based on decision trees. By optimizing the hyperparameters of this model, a minimum classification accuracy of 95.62% has been achieved for workflow states.

(4) The integration of multi-source data with the testing process facilitates not only the determination of test conditions but also the tracing of various parameters during operation, thereby ensuring the consistency of tests and enhancing the credibility of test results.

In summary, this study integrates non-intrusive monitoring technology with multi-source data analysis to construct a multi-source data-driven method for classifying the working states of fabric pilling and linting performance detection. By implementing detailed monitoring and intelligent classification during the detection process, it contributes to enhancing the reliability and accuracy of detection results, thereby playing a role in advancing the field of textile quality control technology.

II. RELATED RESEARCH

A. METHODS AND ISSUES IN FABRIC PILLING PERFORMANCE DETECTION

With the improvement of living standards, the demand for textile quality is increasing. The pilling performance of fabrics is a key indicator in assessing textile quality. However, in the current field of textile quality detection, there are various methods and standards adopted by different countries [8], [9], such as the ASTM D4970 standard in the United States, the ISO 12945 series standards in Europe, and the GB/T 4802 standard in China [10]. This necessitates the selection of appropriate testing standards and methods based on the destination, type of product, and specific requirements of buyers. In this study, fabric pilling and linting tests were mainly conducted using the circular trajectory method and the pilling box method.

To improve the accuracy of detection reports, Dong [11] proposed that enhancing the accuracy of fabric pilling and linting performance evaluation requires strengthening the management of personnel and detection instruments, emphasizing environmental control, and strengthening the management of test results and reports. However, in previous fabric performance detection experiments, the writing of experiment records and reports was done by personnel without sufficient data support, making it impossible to know the specific conditions during the experiment when problems occurred subsequently. By introducing a real-time non-intrusive monitoring system driven by multi-source data, we conducted detailed testing and analysis of the fabric pilling and linting detection process of specimens, achieving comprehensive control over the working status of the detection equipment and the ability to trace various parameters during work based on the working states.

B. MULTI-SOURE DATA PROCESSING TECHNIQUES IN REAL-TIME NIM SYSTEMS

In current technical research, real-time non-intrusive monitoring systems have been widely applied in various fields and have demonstrated advantages in obtaining required information without intervening in the original state of the monitored objects. Li and Dick [12] confirmed the superior performance of the best algorithm through comparative experiments on four non-intrusive multi-label classification algorithms using a real-world household dataset. Additionally, Yin et al. [13] proposed a non-intrusive load monitoring framework based on deep convolutional neural networks, which effectively improves the efficiency of appliance state analysis and residential energy management. These research outcomes convincingly demonstrate that non-invasive monitoring technology can accurately handle and analyze multi-modal data in different industry application scenarios, achieve precise classification and traceability of equipment working states, and reflect the vast application prospects of this technology in the field of textile performance detection.

In the field of textile testing, monitoring the electrical parameters, mechanical vibrations, and sound characteristics of equipment during operation can reflect real-time changes in the testing process, effectively compensating for the deficiencies of traditional manual recording methods and improving the accuracy and traceability of test results. Athanasiadis and Doukas [14] developed a real-time non-intrusive load monitoring system based on active power transient response, achieving high computational and memory efficiency, and accurately identifying equipment states and energy consumption. Hou et al. [15] developed the BuMA respiratory monitoring system, which utilizes microphone arrays, beamforming, and noise cancellation techniques to improve the accuracy of non-contact audio signal monitoring in home environments, further demonstrating the broad application potential of this technology across domains.

Significant progress has been made in feature extraction from diverse data sources such as sound characteristics and electrical parameters, providing a solid foundation for the classification of fabric pilling and linting performance detection working states. Munoli et al. [16] effectively enhanced the accuracy of Visual Question Answering (VQA) systems by employing multi-scale feature extraction and fusion techniques to improve image feature representation and text information portrayal. Singh et al. [17] employ efficient machine learning techniques to extract acoustic features from automotive transmission fault data, establishing a systematic approach to vocal diagnosis of automotive transmission malfunctions. Morenas et al. [18] applied edge machine learning techniques to analyze and successfully classify rotor bar faults in motor current characteristics. These studies demonstrate the excellent performance of feature extraction from sound characteristics and electrical parameters in various application scenarios.

C. DECISION TREE-BASED SUPPORT VECTOR MACHINE MULTI-CLASSIFICATION ALGORITHM

When selecting a classification model for multi-source data features captured by real-time NIM systems, SVM has been widely used in various classification tasks due to its advantages in handling nonlinear relationships, strong generalization ability, and interpretability [19]. Zhao et al. [20] proposed a fabric defect detection method based on the Pyramid Histogram of Oriented Gradients (PHOG) and SVM, demonstrating excellent detection, classification performance, and robustness in actual production departments. Anami et al. [21] compared the performance of SVM and Artificial Neural Networks (ANN) in fabric image defect classification and found that the SVM classifier outperformed ANN in classification rate. Although SVM has been used in the textile field for classifying fabric defect images, its application in classifying detection process states in the textile field is also meaningful.

Decision trees, on the other hand, have excellent performance in training speed and handling mixed data types [22]. Combining SVM with decision trees can improve prediction performance and reduce the risk of overfitting on the basis of their excellent classification performance. Recent research further demonstrates the advantages of combining SVM with decision tree classification algorithms. Rzayeva et al. [23] demonstrated the precision of decision tree and SVM joint modeling in predicting local area network equipment failures. Chen et al. [24] innovatively designed a reverse-merged SVM classification decision tree structure, achieving excellent results in power transformer monitoring and fault diagnosis. Given this, this study draws on this approach, aiming to optimize the classification of fabric pilling and linting performance detection processes by integrating personnel activities, equipment power usage, and instrument sound data using the decision tree support vector machine (DT-SVM) algorithm.

D. CLASSIFICATION METHODS FOR OPERATIONAL STATES

The methods discussed in the referenced literature have been widely applied and validated in other domains, providing valuable insights for our research. Drawing upon the referenced literature, this paper designs and implements an efficient working-state classification system tailored for textile inspection laboratories, leveraging NIM techniques. Inspired by Bo Yang's comprehensive review on lithium-ion batteries (LiBs) State-of-charge (SoC) estimation models, which categorizes six classes with stringent criteria to guide electric vehicles (EVs) performance assessments, our approach similarly aims for high precision and reliability in a different domain. Additionally, Hu Zhengwei's non-intrusive BP-Adaboost neural network-based motor operation state identification technique, which achieves over 96% accuracy, highlights the potential of non-intrusive methods for high-fidelity state recognition. This has influenced our choice of non-intrusive sensing techniques to avoid interference with the subject under test. Moreover, Yoon et al.'s successful detection of intricate occupant activities using a non-intrusive machine learning model augmented with building data has inspired our use of advanced machine learning models for precise monitoring. Therefore, we believe that these validated methods can play a crucial role in enhancing the accuracy and reliability of our research process and results.

III. RESEARCH METHODS

To address the lack of traceability in fabric pilling and linting detection experiments and the need for non-intrusive diagnostics, this paper introduces NIM technology into the field of textile strength testing, constructing a real-time NIM system tailored for fabric pilling detection in a laboratory environment. This system collects and processes a large amount of real-time data on the dynamic operation of detection equipment, including machine power consumption parameters, equipment operating sounds, and experimental personnel behavior, to achieve comprehensive control over the working status of the detection equipment.

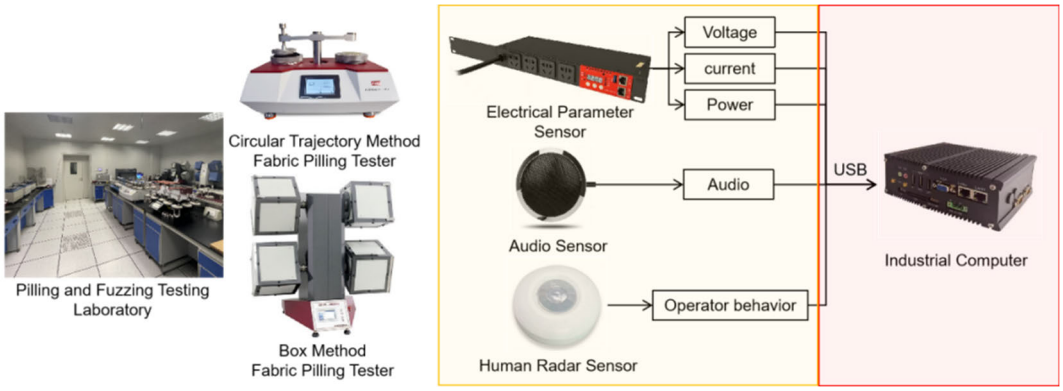

FIGURE 1. Real-time non-intrusive monitoring system.

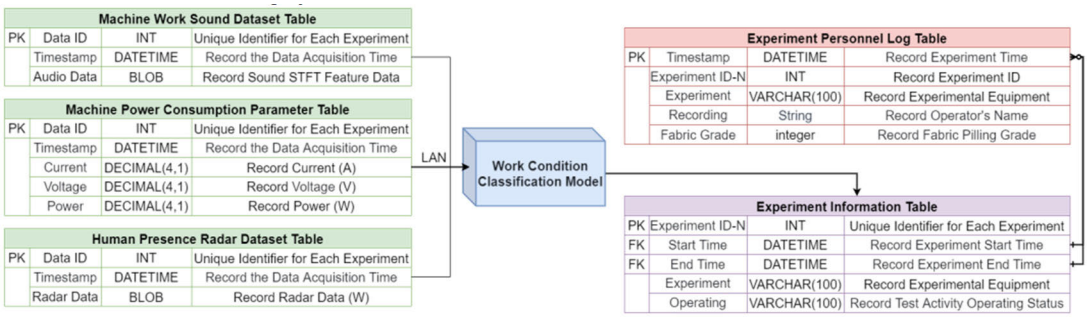

FIGURE 2. Data flow.

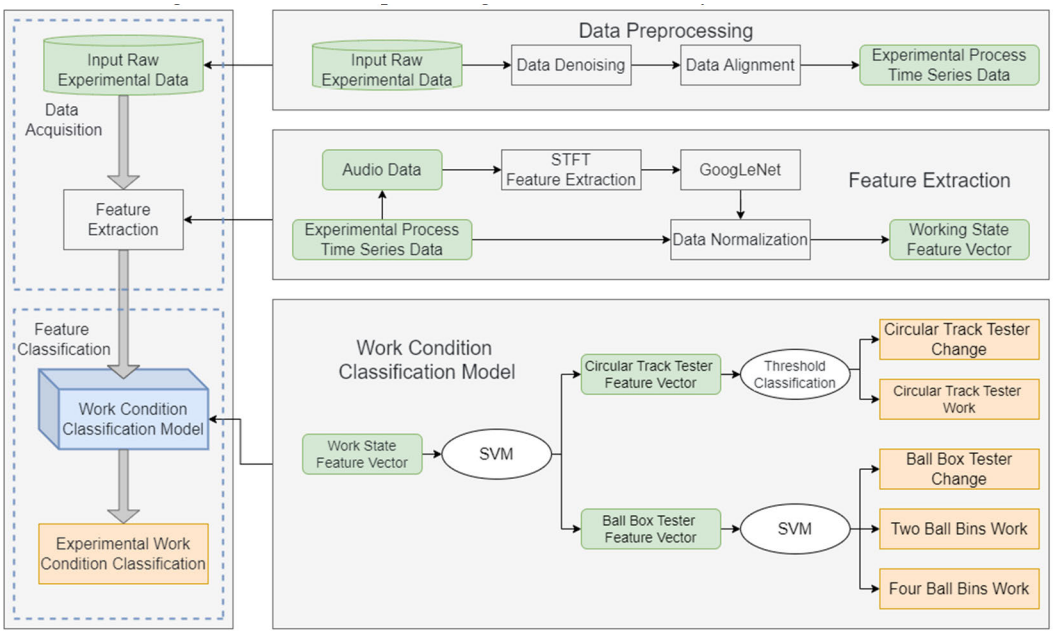

FIGURE 3. Work flow.

A. SYSTEM DESIGN

Given that the internationally recognized flat abrasion test is the Martindale method instead of the circular track method, the present study utilized the circular track method in accordance with the Chinese National Standard 'GB/T 4802.1-2008: Textiles – Evaluation of Fabric Pilling

Performance – Part 1: Circular Track Method' [26], whereas the ball-box method was carried out following the International Standard 'ISO 12945-1-2020: Textiles – Determination of Fabric Propensity to Surface Fuzzing and Pilling – Part 1: Pilling Box Method' [27]. In response, we have devised and executed a real-time, non-intrusive monitoring system within the context of an actual laboratory environment and conforming to prescribed testing standards, depicted in Figure 1. This system continuously collects and processes diverse data sets, encompassing electrical parameters from machinery, sound emissions during equipment operation, and the behavioral actions of the experimenters, thus tackling challenges posed by voluminous and highly redundant data.

Figure 1 presents the architecture of the real-time, NIM system that has been assembled. This system incorporates suitably chosen sensors to collect pertinent data on power consumption characteristics of the experimental apparatus, machinery operation noise levels, and staff activities, all of which undergo initial data filtering and handling on an industrial computer. Datasets from various sensors, each captured at its specific sampling rate, are amalgamated into several database tables, including but not limited to a machine work sound dataset table, a machine power consumption parameter table, and a human presence radar dataset table.

Thereafter, the data from these tables is transmitted via LAN to a dedicated model for work condition classification analysis. A dedicated working condition classification model is applied to analyze this accumulated data, with the instrument's work states being systematically recorded against timestamps within the experiment information table. The experiment information table is linked to the experiment personnel log table through the use of start and end timestamps, thus facilitating the retrospective investigation of diverse issues encountered throughout the experiment by referring to personnel logs, as shown in Figure 2.

In the workflow depicted in Figure 3, experimental data undergo a series of data processing steps, encompassing data acquisition and feature extraction stages, culminating in a detailed classification of the system's operational states using a classification model.

The specific procedures are as follows: Raw time-series data obtained from experiments are initially subjected to extensive preprocessing within an industrial control computer environment, which includes noise reduction and data alignment tasks, thereby ensuring the precision and reliability of the time-series signals during experimentation. Following this thorough preprocessing, the processed time-series data is subsequently uploaded to a computational platform for further analysis.

Given that the DT-SVM model cannot directly classify audio signals, STFT technology is employed to transform the audio data into spectrogram representations. Subsequently, the generated spectrograms are processed using the deep learning model GoogLeNet to extract discriminative audio features.

In order to comprehensively represent the system's operational status, a sliding window mechanism is utilized to extract feature vectors from the multi-modal dataset that reflect changes in the working state after fusion processing. Ultimately, the derived multi-modal operational status feature vectors are fed into a work condition classification model.The model, based on the differential attributes of these features, meticulously categorizes the working states into five distinct classes: circular track tester change, circular track tester work, ball box tester change, and different operating states with either two or four ball-boxes work simultaneously.

B. DATA ACQUISITON

This section describes the testing equipment and monitoring requirements for assessing fabric pilling performance, encompassing machine Power consumption monitoring, machine sound detection, and operator behavior monitoring.

1) MACHINE POWER CONSUMPTION MONITORING

To track the power consumption of the machinery in real-time during the fabric pilling performance test, including parameters such as current, voltage, and power, which reflect the machine's working condition and provide subsequent data support, this study employs electrical parameter monitoring. Referring to the electric parameters during the operation of the pilling tester, the detection apparatus must cover the range of voltage, current, and power during the instrument's functioning, with a voltage measurement accuracy not exceeding 0.1, a current accuracy not exceeding 0.01, and power accuracy not exceeding 0.1. According to 'GB/T 4802.1-2008: Textiles – Evaluation of Fabric Pilling Performance – Part 1: Circular Track Method', the rotational speed is 60±1 revolutions per minute (r/min), and in the 'ISO 12945-1-2020: Textiles – Determination of Fabric Propensity to Surface Fuzzing and Pilling – Part 1: Pilling Box Method', the drum speed is 60±2 r/min, implying that the operating frequencies of both instruments are approximately 1 Hz. Based on the Nyquist theorem, the sampling frequency should be at least twice the highest frequency component of the signal, hence, a sampling rate greater than or equal to 2 Hz is required.

2) MACHINE SOUND DETECTION

The sound frequencies generated by the machine during its operation can serve as an auxiliary indicator of its working status. Considering that the sound frequency ranges of the pilling box and circular track tester are between 100 Hz and 8 kHz, and the primary sound range is 0-3 meters, the sound sensor used in this system should have a collection range not exceeding 3 meters. Following the Nyquist sampling theory, the sampling frequency should be greater than or equal to 16 kHz.

3) OPERATOR BEHAVIOR MONITORING

In the fabric pilling performance testing experiment, monitoring the operators' behaviors ensures the safety and

reliability of the tests and provides classification basis for sample-changing work states. Human radar sensors, compared to other human body sensors, enable non-intrusive, high-precision human detection and tracking without direct contact with the target. Given the sensor layout in the laboratory, the distance between the human radar sensor and the personnel under detection is within 0-1 meter. To meet the requirement for personnel detection distances, the sensor's monitoring range should span 0-1 meter, covering a forward-facing 180° field of view.

C. DATA PROCESSING

1) DATA DENOISING

In the practical process of sensor data acquisition, electrical parameter sensor data is susceptible to various noise interferences, while Boolean output signals from human radar sensors typically do not require filtering treatment. Specifically for electrical parameter sensors, parameters such as current, voltage, and power measurements can be affected by electromagnetic noise generated by operating electrical equipment within the power system.

Drawing inspiration from the noise reduction methodology employing the Kalman filter as reported by Yang Zhang and colleagues in the context of oceanic temperature sensing [30], this study adapts and applies similar principles to electrical parameter sensors operating within laboratory environments. Given that laboratory conditions entail noise profiles that are both more defined and amenable to filtration when contrasted with the intricate dynamics of marine ecosystems, an endeavor has been made to elevate data integrity through the adoption of the conventional linear Kalman filtering algorithm. Initially, a state space model is constructed where the state transition Equation (1) describes how the system's state evolves through a linear dynamic process; the measurement Equation (2) represents the sensor measurements obtained via linear observations [31].

$$x_k = Ax_{k-1} + Bu_k + w_k \tag{1}$$
$$z_k = Hx_k + v_k \tag{2}$$

In the equation: represents the prior estimate of the state; denotes the state transition matrix; signifies the input matrix; stands for the external input;is the sensor measurement; represents the process noise; and refers to the measurement noise.

Based on this model, we first use the previous state estimation and the system model to predict the current state, obtaining the state prediction Equation (3) and the corresponding predicted covariance matrix Equation (4):

$$\hat{x}_{k|k-1} = A\hat{x}_{k-1|k-1} + Bu_k \tag{3}$$
$$P_{k|k-1} = AP_{k-1|k-1}A^T + Q \tag{4}$$

In the equation: represents state prediction, is the covariance matrix of the state estimation, and denotes the covariance matrix of the process noise.

Next, combining the current measurement, we calculate the Kalman gain Equation (5) to update the state estimate Equation (6) and the updated covariance matrix Equation (7):

$$K_k = P_{k|k-1}H^T \left(HP_{k|k-1}H^T + R\right)^{-1} \tag{5}$$
$$\hat{x}_{k|k} = \hat{x}_{k|k-1} + K_k \left(z_k - H\hat{x}_{k|k-1}\right) \tag{6}$$
$$P_{k|k} = (1 - K_k H) P_{k|k-1} \tag{7}$$

In the equation: represents the Kalman gain,and is the covariance matrix of the measurement noise.

Through this iterative cycle of prediction-update steps, the Kalman filter recursively optimizes the state estimation and effectively removes electromagnetic interference and other noise components, thereby significantly improving the quality of the electrical parameter sensor data. This method not only upgrades data quality but also ensures the reliability and reproducibility of scientific research results. It effectively mitigates the impact of noise on experimental outcomes, allowing experimental data to more accurately reflect real conditions, thus facilitating robust and reliable conclusions.

2) AUDIO DATA DIMENSIONALITY REDUCTION AND FEATURE EXTRACTION

In the classification of machine working audio signals, raw high-dimensional audio data pose challenges due to their time-series nature with rich frequency components and non-stationary characteristics. Directly employing such high-dimensional data for SVM training would significantly increase computational complexity, and unprocessed audio data typically do not meet the requirement for comparability and standardization that SVMs generally demand. Hence, this study employs dimensionality reduction techniques to reduce computational burden, eliminate noise, and remove redundant information, thereby enhancing model generalizability and preventing overfitting.

To embed the audio signal effectively into the SVM framework, we first transform it into a time-frequency spectrogram using STFT to jointly represent temporal and frequency information. Given the inherent non-stationarity in industrial machine working audio signals affected by mechanical noise, environmental changes, etc., direct application of Fourier Transform fails to adequately capture its dynamic features evolving over time. Thus, STFT is adopted, which approximates stationarity within short-time windows and extracts instantaneous frequency characteristics as defined by Equation (8):

$$STFT\,(t,f) = \int_{\infty}^{\infty} x\,(\tau) w\,(\tau - t)\, e^{-j2\pi f \tau} d\tau \tag{8}$$

In the equation: represents the input function, denotes the window function, represents a complex exponential term that signifies a complex sinusoidal wave of frequency.

During the experimental process, the audio signal is divided into multiple overlapping time-window segments, and STFT is performed on each segment to obtain spectral features within those windows. The specific parameter settings involve a 1-minute window size and a 5-second sliding step strategy, allowing systematic extraction of key

state-related features from the non-stationary audio data. Based on this, the resulting time-frequency spectrograms are categorized into five class labels: Non-Operational State (Label 0), Circular Track Operating State (Label 1), Ball-Box Sample change State (Label 2), Two Ball-Boxes Work Simultaneously (Label 3), and Four Ball-Boxes Work Simultaneously (Label 4).

For effective analysis and classification of the extracted time-frequency spectrograms, this research utilizes the GoogLeNet convolutional neural network model. The core innovation of GoogLeNet lies in its carefully designed Inception module structure, as shown in Figure 4. This module processes multiple scales of features in parallel through integrating various kernel sizes (including 1×1, 3×3, and 5×5 convolutions) and max pooling operations, stacking and fusing them to build a multi-level, multi-scale feature representation space. This design enables the network to simultaneously capture crucial features at different spatial resolutions and further refine these into abstract, richly-layered features, significantly enhancing its representation capability for complex audio patterns.

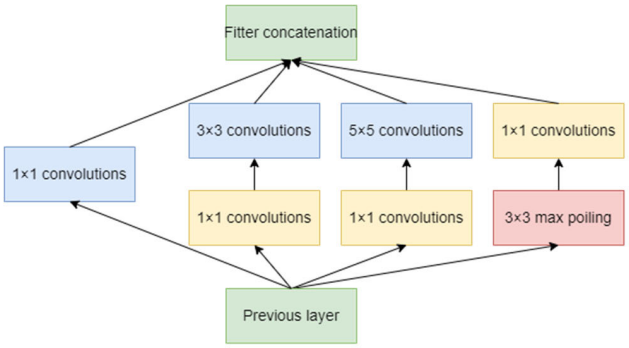

FIGURE 4. Inception module.

Notably, the Inception module embraces a lightweight design philosophy, effectively reducing the number of network parameters. This simplifies the training process, enhances computational efficiency, and allows the model to handle larger image datasets under limited computational resources. Additionally, embedded auxiliary classifiers distributed across different intermediate layers in GoogLeNet provide extra gradient feedback, accelerating the overall network training process while helping alleviate the vanishing gradient problem in deep learning networks, thus improving both training efficiency and model performance.

Of particular significance, GoogLeNet excels in dimensionality reduction. Its sparsely connected Inception modules cleverly leverage parallel processing of input features using different-sized convolution kernels; the 1×1 convolution layer plays a critical role in reducing computational complexity and decreasing dimensions, while global average pooling further compresses the depth and dimensions of feature maps, significantly lowering the model's parameter count and computational load. This efficient design ensures that GoogLeNet can maintain a compact model dimensionality while enhancing computation efficiency and performance, particularly suitable for tasks involving high-dimensional audio feature representations with rich spatiotemporal information.

Finally, the results after the above processing and classification are recorded in the ''Machine Work Sound Dataset Table'' to meticulously track and differentiate sound feature differences during various operational states of the equipment, providing robust data support for subsequent machine condition monitoring and fault diagnosis tasks.

3) DATA SYNCHRONIZATION

In real-time NIM systems, ensuring temporal consistency among data collected from multiple sensors is a core task. This system integrates diverse parameters such as power usage metrics, machine sound feature analysis, and operator behavior pattern recognition. Due to the inherent differences in sampling frequencies across various sensors, which lead to asynchronous timestamps, direct comparison and analysis can be misleading due to data inconsistency. To address this issue, given the significant discrepancies in sampling frequencies and conversion intervals among electrical parameter, human radar, and sound sensors, along with the extensive time span covered by the database records, this study employs a sliding time window alignment method partitioned into discrete time periods to simplify the overall synchronization process.

After effectively filtering out intermittent noise interference during preprocessing, we devised a sliding window strategy based on the minimum common sampling frequency, setting a 1Hz time interval, to progressively align all data points in timestamp order. For those sensors with sampling rates significantly higher than 1Hz, including human radar, power consumption sensors, and sound sensors, we employed the method shown in Equation (9) to perform aggregation operations for down-sampling alignment:

$$Average_i = \frac{1}{|W|} \sum\nolimits_{j \in W_i} S_j \tag{9}$$

In the equation: W represents the size of the sliding window, W_i refers to the set of all data points within the i-th sliding window, and j denotes the measured value of the j-th original data point within window W_i.

This approach ensures precise temporal matching of data from different sampling frequencies across various sensors, thereby guaranteeing the effectiveness and accuracy of the real-time NIM system.

4) DATA NORMALIZATION

In this research, Boolean data output by the human radar sensor, due to its binary nature, does not require normalization preprocessing. However, for other types of continuous data within the sliding windows, prior to applying SVM for classification tasks, we adopted a normalization strategy to eliminate scale differences between features that could

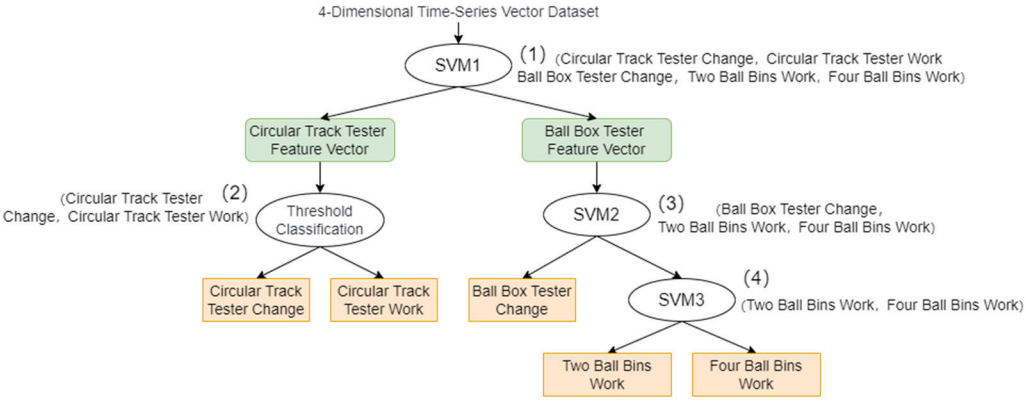

FIGURE 5. Multi-class flowchar.

influence decision boundaries and ensure consistent model attention to all features.

The chosen normalization method was Min-Max scaling, favored for its intuitive simplicity and retention of the original data distribution shape. Although under certain extreme conditions, this method may compress outliers into a smaller interval, at the current experimental stage, having successfully removed distinct discrete data points, Min-Max scaling proved suitable and effective in this specific context. In practice, for each individual sliding window, we separately calculated the minimum and maximum values of each feature dimension and then used Equation (10) to map the average values of all features within the sliding window onto the [0,1] interval, thus achieving standardized data processing.

$$X = \frac{X - min}{max - min} \tag{10}$$

Moreover, to optimize memory usage and focus on the core analytical areas, only normalized data within the sampled windows were retained, while the rest were discarded.

5) STATE CLASSIFICATION

For the more complex problem of equipment state classification involving multiple dimensions such as power consumption parameters, sound signals, and personnel behaviors, this study employs the SVM algorithm. SVM has demonstrated exceptional performance in solving high-dimensional space problems, particularly when dealing with high-dimensional data and limited sample sizes, effectively reducing the risk of overfitting. Leveraging kernel mapping techniques, SVM transforms originally non-linearly separable problems into linearly separable ones in higher-dimensional spaces, successfully addressing complex nonlinear relationships among features.

This research combines the intuitive interpretability of decision trees with the high-dimensional classification efficiency of SVM to devise an effective strategy for classifying the states of machinery used in fabric pilling and fuzzing performance testing. The detailed steps are as follows:

(1) A four-dimensional time-series vector dataset is initially input into SVM1, which serves to segment the overall operation states of the Circular Track Tester and Ball Box Tester. This step discerns between the 'Circular Track Tester Change' state and the 'Circular Track Tester Work' state.

(2) The 'Circular Track Tester Work' state's refined feature vector undergoes classification using a threshold classifier. This step differentiates between the 'Circular Track Tester Change' state and 'Circular Track Tester Work', based on Boolean features indicating operator proximity to the instrument.

(3) Similarly, the work state feature vector for the 'Ball Box Tester' is passed through SVM2 to accurately classify it into the 'Ball Box Tester Change' state and the 'Ball Box Tester Work' state.

(4) Once the Ball Box Tester's work state has been clearly categorized, the corresponding data is fed into SVM3 to further discriminate between two different 'Two Ball Bins Work' states and a state where all 'Four Ball Bins' are operating simultaneously

The specific classification process is illustrated in Figure 5: Multi-Class Flowchart.

The threshold classifier for the circular trajectory work state primarily involves judgment of the operator's activity status, with threshold values based on Boolean features indicating operator presence near the instrument.

Regarding the selection of the kernel function for the SVM classifiers, given that the input features consist of four dimensions—sound, electrical parameters, and personnel activities—which exhibit nonlinear relationships and have complex, irregular distributions, we opted for the Gaussian radial basis function (RBF) kernel due to its high flexibility and strong capacity for modeling nonlinearities. The employed Gaussian kernel function is defined by Equation (11):

$$K(x, y) = exp(\frac{\| x - y \|^2}{-2\sigma^2}) \tag{11}$$

TABLE 1. Comparison of fabric pilling test machine parameters.

Parameter	YG511N-4 Box-Type Pilling Tester	YG502N Fabric Pilling Tester
Power Supply Voltage	AC220V	AC220V
Operating Power	120W	90W
Current	6A	6A
Frequency	50Hz	50Hz
Motion Path	40mm Circular Trajectory	-
Speed	60±1r/min	60r/min

TABLE 2. Situation awareness sensor parameters.

Sensor Type	Measurement Range	Coverage	Precision	Sampling Frequency
Human Radar	0m - 10m	150° Conical	-	10 Hz
Audio	0-5m	Omnidirectional	40±3dB	16K Hz
Voltage	110V - 240V	-	1V	2 Hz
Current	0A - 10A	-	10mA	2 Hz
Power	0W - 2500W	-	0.1W	2 Hz

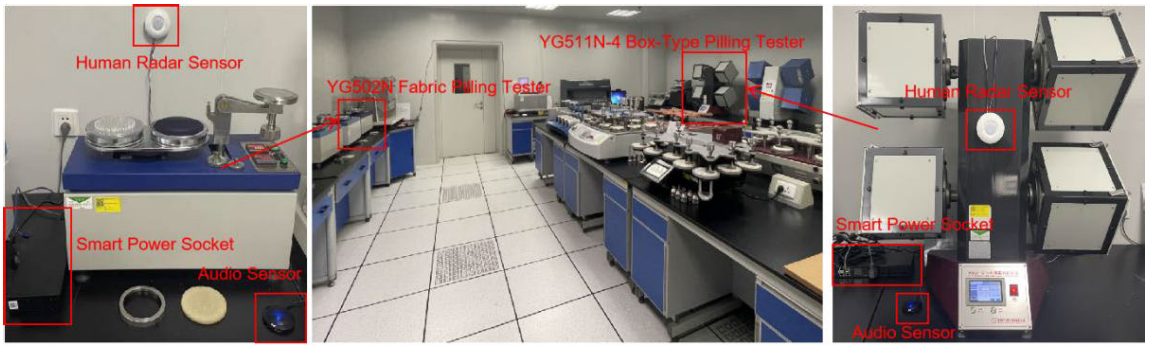

FIGURE 6. On-site deployment diagram.

In the equation: $\| x - y \|$ represents the squared Euclidean distance between sample x and y.σ denotes the bandwidth, which is an adjustable parameter in the Gaussian kernel function, controlling the range of distribution that samples are mapped to in higher-dimensional space.

IV. EXPERIMENT DESIGN

This section provides a comprehensive overview of the experimental process for fabric pilling and fuzzing performance evaluation based on multi-source data, encompassing the experimental environment, instrument configurations, sensor parameter settings, dataset construction, visualization analysis, and culminating with an in-depth discussion of the optimization strategies for the DT-SVM model.

A. INTRODUCTION TO THE EXPERIMENT ENVIRONMENT

The research was conducted in collaboration with the Zhejiang Institute of Quality Inspection for Light Industrial Products. The experimental instruments were supplied by Nantong Hongda Experimental Instrument Co., Ltd. For the box method testing, a YG511N-4 Box-Type Pilling Tester was employed, while the circular track method utilized a YG502N Fabric Pilling Tester. The detailed technical specifications of these instruments are presented in Table 1.

Additionally, the experimental platform included a high-performance computer equipped with an Intel Core i7-6700HQ processor and an NVIDIA GeForce GTX 1060 GPU. To collect diverse data, several sensors were deployed, such as a sound sensor (Sony Capacitive Microphone), a human

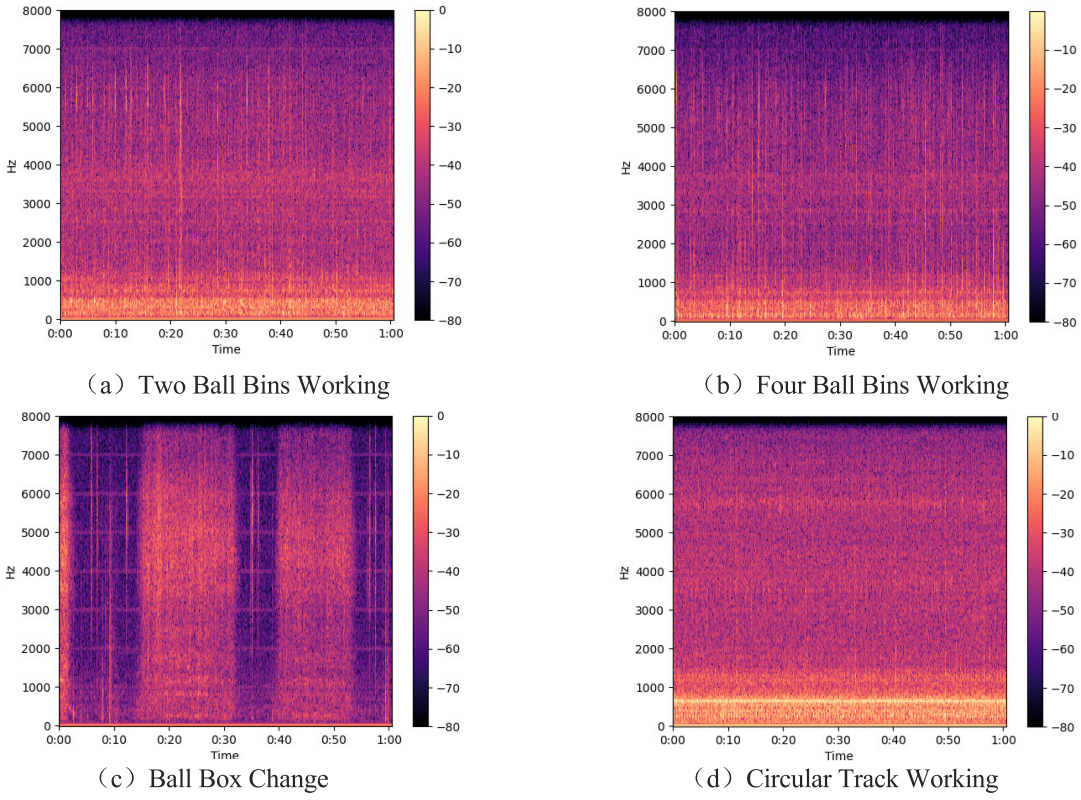

（a）Two Ball Bins Working

（b）Four Ball Bins Working

（c）Ball Box Change

（d）Circular Track Working

FIGURE 7. STFT spectrogram.

radar sensor (Zetai 485 Human Presence Sensor), and power consumption sensors (GWGJ Intelligent PDU). The specific signal parameters for these sensors are listed in Table 2.

The data acquisition frequency set by the data collection devices, as indicated in Table 2, effectively ensures the completeness and high accuracy of data collection, thereby guaranteeing the intact reproduction of system processes during subsequent analyses or retrospectives.To ensure comprehensive reliability of the experiment, the focus was placed on detailing the laboratory environment, which featured advanced computing equipment and the strategic placement and parameter configuration of various sensors. Figure 6 presents a clear layout of sensor placements, critical for understanding experimental conditions and contextualizing the results.

B. COMPARATIVE EXPERIMENT ON SOUND FEATURE EXTRACTION

By examining STFT-generated spectrograms of collected audio features, distinct differences in sound characteristics were revealed under various operational states of the fabric pilling detection equipment, including non-operational states, ball bin replacement operations, synchronous operation of two ball bins, asynchronous operation of four ball bins, and circular track work. As shown in Figure 7, each working condition presents unique temporal-frequency patterns.

Observations from the experiment showed that when the rolling bins were operational, due to the large volume and high rotation speed of the drums, the frequency fluctuations in the generated sound signals were significantly more intense and frequent compared to the steady-state operation of the circular track mode. Conversely, sound frequency changes in the circular track work were smoother and more continuous. A comparison of scenarios where four ball bins worked simultaneously versus two ball bins synchronously demonstrated that the former's time-frequency spectrograms exhibited denser and more amplitude-varying features due to the asynchronous nature of the ball bins. In the ball box change phase, identifiable acoustic signatures from the interaction between abrasives and fabric samples could be discerned from the spectrogram in Figure 7(c), whereas during regular ball bin work, the primary captured sounds were related to mechanical noise from the rotating machinery.

Table 3 summarizes the durations of audio data samples collected under different states. Notably, the audio samples for non-working states and ball bin changes were shorter, especially those for the changeover operations. To address this issue, sliding window techniques were adopted, applying suitable window strides to the audio data according to each state's specifics, aiming to balance the number of converted STFT images across all working states. By preprocessing all raw audio data in this manner, converting them into spectrograms, and meticulously labeling them according to their

corresponding operational states, a comprehensive sound feature dataset was constructed.

TABLE 3. Situation awareness sensor parameters.

Operating State	Total time（s）
Power off	1356
Circular Track Work	1893
Ball Box Change	356
Two Ball Bins Work	2235
Four Ball Bins Work	2126

Finally, GoogLeNet convolutional neural network architecture was further applied to classify these image-based sound features, aiming to distinguish the unique sound patterns associated with each operational state.

C. DATASET AND DATA VISUALIZATION

In the actual instrument operation and data collection process, the number of samples for different states in the dataset varied. An imbalance in the amount of data associated with a particular label could negatively affect the SVM classification performance. Excessive amounts of data can lead to overfitting, where the model becomes overly complex and fits noise in the training data rather than the underlying pattern. Conversely, insufficient data can cause underfitting, where the model is too simple and fails to capture the complexity of the problem at hand. In cases of class imbalance, the model may tend to favor majority classes and struggle to learn patterns from minority classes.

TABLE 4. Dataset.

Category	Train	Test
Circular Track Change	2015	229
Circular Track Work	1725	190
Ball Box Change	1817	199
Two Ball Bins Work	2018	224
Four Ball Bins Work	2063	228

In our case, the changeover state had the least amount of data for both working instruments, while the working state data for the ball box tester was notably abundant due to typical operating times ranging from 2 to 4 hours. To mitigate the effects of overfitting and underfitting on the classification model, data augmentation was performed on the changeover states for both the circular track and ball box testers, while undersampling was applied to the working state data of the ball box tester. This ensured that each state had approximately equal representation within the dataset.

The final dataset comprised 10,708 records, which were labeled as ‘Circular Track Change’, ‘Circular Track Work’, ‘Ball Box Change’, ‘Two Ball Bins Work’, and ‘Four Ball Bins Work’, represented by numerical labels 0, 1, 2, 3, and 4, respectively. The dataset was randomly partitioned, with 10% of the total data designated as the testing set. Table 4 presents this balanced and partitioned dataset.

Figures 8 and 9 illustrate the variations in multiple parameters and state changes during the fabric pilling and fuzzing tests using the ball box and circular track methods. Figure (a) shows voltage changes, (b) displays power changes, (c) represents the presence or absence of personnel, and (d) indicates whether there was machine-generated sound. Different background colors denote the various states without considering environmental anomalies, where light red represents the power off state, yellow denotes standby, orange signifies the change state, green represents the two ball bins work state, purple indicates the four ball bins work state, and cyan represents the circular track work state.

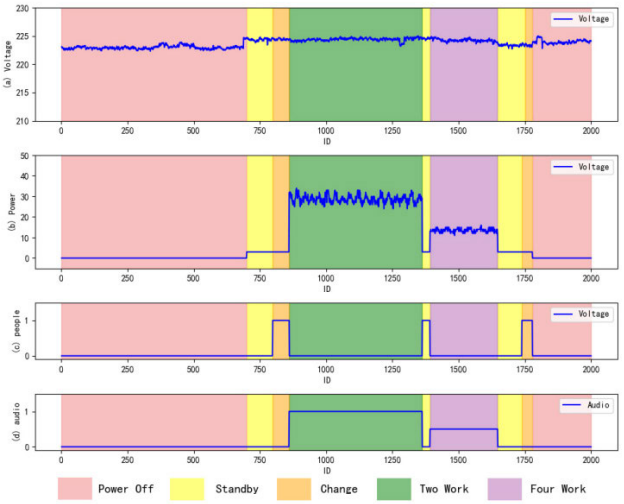

FIGURE 8. Ball box teser visualization diagram.

D. DT-SVM MODEL OPTIMIZATION

Hyperparameters are parameters manually set by researchers before the model training process begins and do not get learned from the training data. They play a critical role in determining the structure and learning process of the model, significantly influencing its learning capacity, complexity, and generalization ability. The selection of hyperparameters directly impacts the model’s behavior and performance, with different configurations potentially leading to substantial differences. In the classification problem discussed in this paper, the main hyperparameters that critically affect the model’s performance include the kernel function, regularization parameter C, and scale parameter γ.

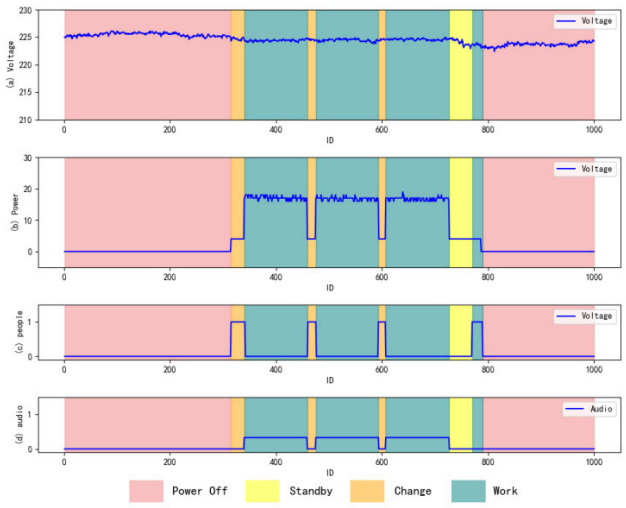

FIGURE 9. Circular track tester visualization diagram.

Given that we employed a DT-SVM model suitable for multi-class scenarios, we selected the Gaussian radial basis function (RBF) kernel due to its strong nonlinear mapping capabilities, which are apt for complex classification tasks. However, the crucial aspect for this model lies in optimizing the combination of the regularization parameter C and the scale parameter γ to achieve optimal classification results. To this end, this study utilized cross-validation, using accuracy as the core metric to evaluate model performance and identify the optimal hyperparameter combination. The formula for calculating accuracy is shown as Equation (12):

$$Accuracy = \frac{TP + TN}{TP + TN + FP + FN} \times 100\% \quad (12)$$

In the equation: *TP* stands for True Positives, *TN* represents True Negatives, *FP* denotes False Positives, and *FN* signifies False Negatives.

Through cross-validation optimization of the SVM model under various combinations of the regularization parameter C and the kernel function parameter γ, we recorded the classification accuracies. We then compiled those results with accuracies exceeding 90% into Table 5.

The results showed that when the kernel function parameter γ was set to 0.5, and the regularization parameter C was set to 0.1, the model achieved the highest classification accuracy at 97.17%. This outcome effectively demonstrates the importance of judiciously selecting hyperparameters for enhancing the model's performance.

V. EXPERIMENTAL RESULTS AND ANALYSIS

A. EXPERIMENTAL STATE CLASSIFICATION AND HYPOTHESES

The experiment is set with five states: 'Circular Track Change', 'Circular Track Work', 'Ball Box Change', 'Two Ball Bins Work', and 'Four Ball Bins Work'. It is hypothesized that in the 'Circular Track Change' and 'Ball Box Change' states, the sensor detects significantly lower motion frequency and continuity compared to the working states, with higher power readings but lower audio features. In the 'Circular Track Work' state, the sensor is expected to detect continuous circular motion, with moderate power readings and audio features. For the 'Two Ball Bins Work' and 'Four Ball Bins Work' states, the sensor should detect dual and quadruple periodic motion patterns, with higher activity frequencies, power readings, and audio features. Specific data are provided in Table 6.

TABLE 5. Cross-validation accuracy.

kernel	C	γ	Accuracy (%)
	0.01	0.1	92.70
	0.01	1	91.25
	0.01	0.5	91.09
rbf	0.1	0.1	92.70
	0.1	0.5	97.17
	0.5	0.01	91.34
	1	0.01	92.41

TABLE 6. State classification and hypothesized parameterst.

Category	Power	Audio	People	Voltage
Circular Track Change	17±2	0	0	
Circular Track Work	4±1	0.25	1	
Ball Box Change	4±1	0.5	0	>220
Two Ball Bins Work	14±2	0.75	1	
Four Ball Bins Work	30±5	1	1	

Here, 'People' denotes a binary value captured by the Human Radar Sensor, 'Power' refers to the power range recorded by the Power Sensor, and 'Audio' signifies the audio features derived from the STFT analysis conducted in the 'Comparative Experiment on Sound Feature Extraction'.

B. EVALUTION METRICS

When assessing model performance, relying solely on accuracy as a single metric may not fully reflect the model's behavior when dealing with imbalanced datasets. In cases where class distributions are uneven, the model might tend to predict samples from the majority class while neglecting its ability to identify minority class instances. Hence, using a combination of multiple evaluation metrics is particularly crucial.

FIGURE 10. Comparative experiment on audio feature extraction.

TABLE 7. Model classification experiment.

Model	VGGNet16			GoogLeNet			DenseNet		
	PRC	REC	F1	PRC	REC	F1	PRC	REC	F1
Power off	1.00	0.95	0.97	0.95	1.00	0.97	1.00	0.99	0.99
Circular Track Work	0.94	1.00	0.97	1.00	0.94	0.97	0.98	1.00	0.99
Ball Bin Change	1.00	1.00	1.00	1.00	1.00	1.00	1.00	1.00	1.00
Two Ball Bins Work	1.00	1.00	1.00	1.00	1.00	1.00	1.00	1.00	1.00
Four Ball Bins Work	1.00	1.00	1.00	1.00	1.00	1.00	1.00	1.00	1.00
AVG	0.988	0.990	0.988	0.990	0.988	0.992	0.996	0.998	0.996
FPS		0.18			0.54			0.14	
Accuracy		97.29%			98.79%			99.69%	

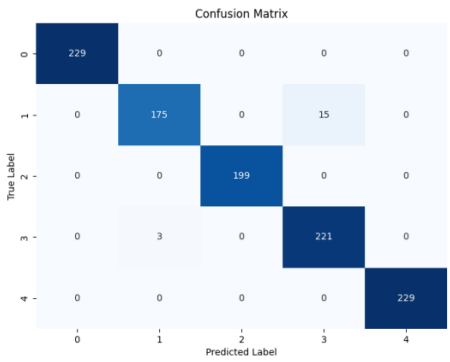

FIGURE 11. Confusion matrix.

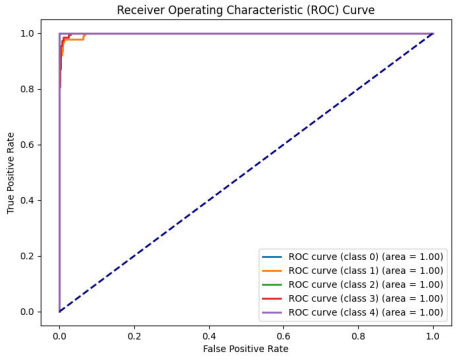

FIGURE 12. ROC curve.

Precision (PRC) and Recall (REC) are two core parameters indispensable for evaluating the performance of classification models. Precision measures the proportion of actual positive samples among those predicted as positive by the model, as shown in Equation (13):

$$\mathrm{PRC} = \frac{TP}{TP + FP} \times 100\% \tag{13}$$

The recall quantifies how many of the truly positive samples were correctly identified, revealing the model's coverage of genuine positives, with its formula given in Equation (14):

$$\mathrm{REC} = \frac{TP}{TP + FN} \times 100\% \tag{14}$$

In the context of class imbalance, we introduce F1-score(F1) as a comprehensive evaluation metric that

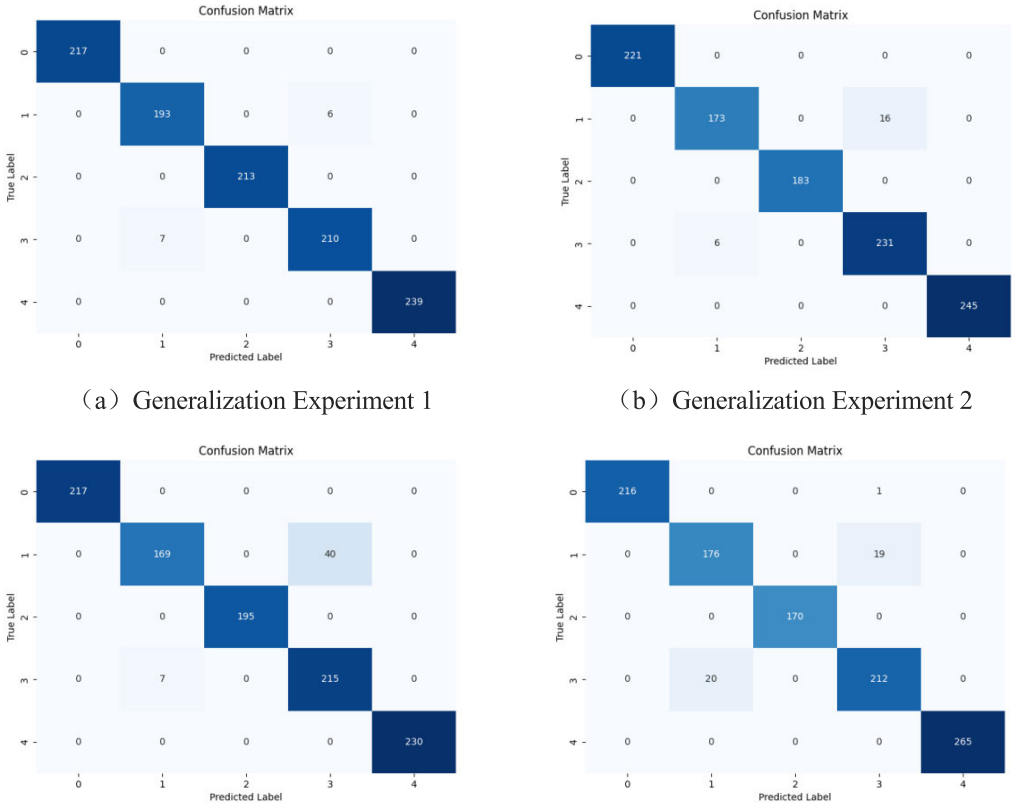

（a）Generalization Experiment 1

（b）Generalization Experiment 2

（c）Generalization Experiment 3

（d）Generalization Experiment 4

FIGURE 13. Enlarged data confusion matrix.

balances precision and recall; it is the harmonic mean of precision and recall, aiming to consider both the preciseness and completeness of the model, calculated according to Equation (15):

$$\mathrm{F1} = 2 \times \frac{PRC \times REC}{PRC + REC} \tag{15}$$

The Receiver Operating Characteristic Curve (ROC) further illustrates the model's discriminative ability between positive and negative samples at different thresholds. An ideal ROC curve should be as close as possible to the top-left corner, indicating high recall with low false positive rate. The larger the Area Under the Curve (AUC), the better the model's performance.

C. AUDIO FEATURE EXTRACTION COMPARISON EXPERIMENT

The audio feature extraction comparison experiment evaluated the differences in performance among several typical CNN architectures—VGGNet 16, GoogLeNet, and DenseNet—using metrics such as Accuracy, PRC, REC, and F1 scores. As shown in Table 7, the confusion matrices for each model architecture on the test set are depicted in Figure 10. The DenseNet model achieved the highest classification accuracy of 99.69%, but considering its slower processing speed compared to GoogLeNet, which maintained a relatively high accuracy of 98.79% while tripling its processing speed, this study chose to employ the GoogLeNet architecture for classifying audio STFT spectrograms and integrating the classification results into the machine working sound data table for subsequent analysis.

D. DT-SVM CLASSIFICATION EXPERIMENT

During the experimental phase, we employed several key evaluation metrics to assess the DT-SVM model's performance under different operating conditions. Figure 11 presents the corresponding confusion matrix, and Table 8 lists the precision, recall, and F1-scores, reflecting the model's classification performance for each work state. Notably, the DT-SVM model demonstrated overall strong performance, achieving an overall accuracy rate of 98.32%.

To provide a more intuitive assessment of the model's discriminative capability and overall performance, this research plotted the ROC curve, shown in Figure 12 By observing the AUC value, we can obtain a comprehensive evaluation of the model's ability to classify positive and negative samples under varying threshold settings.

TABLE 8. DT-SVM model performance metrics.

Model	DT-SVM		
	PRC	REC	F1
Circular Track Change	1.00	1.00	1.00
Circular Track Work	0.98	0.92	0.95
Ball Bin Change	1.00	1.00	1.00
Two Ball Bins Work	0.94	0.99	0.96
Four Ball Bins Work	1.00	1.00	1.00
AVG	0.984	0.982	0.982
Accuracy (%)		98.32	

E. GENERALIZABILITY EXPERIMENT

Despite the original dataset containing 10,708 samples, due to the limited amount of training data, the model may not fully capture the complex characteristics of the entire data distribution, thus limiting its generalization capacity. When trained on small sample datasets, models often overfit, performing well on the training set but showing poor generalization performance on the testing set.

To address this issue, we augmented the fabric pilling performance detection dataset with additional multi-source data collected across four sets of records equivalent in scale to the original experiments. By increasing the number of training data, the model was exposed to a more diverse range of samples, which helped it learn and capture invariant features in the data better, thereby enhancing its adaptability to different situations. Moreover, introducing sample diversity also helps mitigate the model's tendency to overfit specific patterns within the training set, improving its ability to handle novel and unknown scenarios, effectively reducing the risk of overfitting.

Upon retraining the model with the expanded dataset using the previously determined optimal hyperparameters, the accuracy rates for each state reached 98.80%, 97.95%, 95.62%, and 96.29%, respectively. The corresponding confusion matrix is displayed in Figure 13.

VI. CONCLUSION AND OUTLOOK

This paper proposes a multi-source data-driven method for classifying the operational states of fabric pilling performance testing, tailored to real-world laboratory environments. The approach utilizes an advanced, real-time NIM system to collect and analyze a variety of data sources including electrical parameters, operator behavior, and sound data. The study employs suitable noise reduction techniques, sliding window alignment, and feature extraction methods, combined with threshold-based classification and a SVM algorithm using decision trees, successfully achieving precise categorization and traceable diagnostics of the fabric pilling performance testing process.

In the experimental setup, we provide detailed descriptions of the configurations of various instruments and sensor parameter settings. Experimental results demonstrate that the proposed multi-source data-driven methodology performs well in handling class imbalance problems. Through cross-validation optimization and selecting appropriate hyperparameters, the final model achieves high accuracy levels across different operating conditions, with a peak accuracy rate of 97.17%, and exhibits strong generalization capability. Upon expanding the dataset, the lowest accuracy achieved by the model for any state was 95.62%, substantiating the effectiveness and reliability of this method.

Despite achieving preliminary results, this study still confronts several limitations and uncovers ample prospects for enhancement and further exploration. To address these, succeeding investigations can concentrate on several pivotal avenues: firstly, broadening the scope of feature dimensions to facilitate a more nuanced differentiation of operational statuses, specifically in pinpointing and categorizing salient signals of abnormal operations, thereby augmenting the diagnostic precision for system malfunctions. Concomitantly, as we enrich feature dimensions, the modernization of data acquisition mechanisms is indispensable, not solely to amplify dataset sizes and hasten computational velocities, but also to ascertain prompt anomaly alerts, circumventing delayed discrepancy identifications post-operation.

Furthermore, the exploration of deep learning frameworks for constructing end-to-end learning ecosystems is advocated, to better accommodate the intricacy and variability inherent in diverse data streams. Alongside, the quest for efficacious techniques in feature extraction must be intensified to bolster the accuracy and resilience of our models.

We are committed to addressing these issues in our subsequent research and encourage future scholars venturing into similar domains to tackle these existing limitations proactively.

Zooming out to a broader perspective, validating the adaptability of our methodology across a spectrum of textile quality assessment scenarios forms a cornerstone of our long-term strategy, aiming to affirm its extensive practicality and validity. Amidst the swift advancements in the Internet of Things (IoT) and 5G communication landscapes, devising schemes for real-time surveillance and remote, intelligent analytical capabilities within detection systems emerges as a pivotal agenda for upcoming studies, steering us towards the profound digitalization and intelligent metamorphosis of the textile sector.

ACKNOWLEDGMENT

The authors gratefully acknowledge the valuable contributions and support provided by Xiaohang Fu, Liegang Han, XiaoHong Jin, Zhu Ming, and Shousai Chen during the course of this research. Their expertise and efforts were instrumental to the successful completion of this study.

REFERENCES

[1] S. Guan, D. Liu, L. Hu, M. Lei, and H. Shi, "Evaluation method of fabric pilling grades based on saliency-based deep convolutional network," *Textile Res. J.*, vol. 93, nos. 13–14, pp. 2980–2994, Jan. 2023, doi: 10.1177/00405175221149678.

[2] Y. Y. Huang and K. L. Dong, "Assessment of pilling severity for color fabrics based on homomorphic filtering," *Prog. Textile Sci. Technol.*, pp. 29–34, Nov. 2021, doi: 10.19507/j.cnki.1673-0356.2021.11.008.

[3] X. Dong, T. Xing, and G. Chen, "Improving the anti-pilling performance of cellulose fiber blended knitted fabrics with 2,4,6-trichloropyrimidine treatment," *Coatings*, vol. 10, no. 10, p. 969, Oct. 2020, doi: 10.3390/coatings10100969.

[4] J. Wu, L. Wang, Z. Xiao, L. Geng, F. Zhang, and Y. Liu, "Wool knitted fabric pilling objective evaluation based on double-branch convolutional neural network," *J. Textile Inst.*, vol. 112, no. 7, pp. 1037–1045, Jul. 2021, doi: 10.1080/00405000.2020.1821984.

[5] J. Wu, Q. Liu, Z. Xiao, F. Zhang, and L. Geng, "Objective rating method for fabric pilling based on LSNet network," *J. Textile Inst.*, vol. 115, no. 4, pp. 535–543, Apr. 2024, doi: 10.1080/00405000.2023.2201531.

[6] T. Chen, H. Qin, X. Li, W. Wan, and W. Yan, "A non-intrusive load monitoring method based on feature fusion and SE-ResNet," *Electronics*, vol. 12, no. 8, p. 1909, Apr. 2023, doi: 10.3390/electronics12081909.

[7] P. A. Schirmer and I. Mporas, "Non-intrusive load monitoring: A review," *IEEE Trans. Smart Grid*, vol. 14, no. 1, pp. 769–784, Jan. 2023, doi: 10.1109/tsg.2022.3189598.

[8] Y. Teng, Y. Xu, and G. Li, "Reflections on fabric pilling performance testing methods," *China Fiber Inspection*, pp. 51–53, Feb. 2022, doi: 10.14162/j.cnki.11-4772/t.2022.02.015.

[9] X. F. Tang, "Investigation on fabric pilling detection methods and testing details," *China Fiber Inspection*, pp. 86–87, Jun. 2022, doi: 10.14162/j.cnki.11-4772/t.2022.06.005.

[10] Y. Wang, Z. Huang, and B. Li, "Analysis of differences between standards for fabric pilling and hairiness testing methods," *China Fiber Inspection*, pp. 90–92, Nov. 2021, doi: 10.14162/j.cnki.11-4772/t.2021.11.027.

[11] H. L. Dong, "Factors affecting the accuracy of textile pilling evaluation results," *Textile Test. Standards*, vol. 9, pp. 9–11, Feb. 2023, doi: 10.19391/j.cnki.cn31-2117.2023.01.009.

[12] D. Li and S. Dick, "Non-intrusive load monitoring using multi-label classification methods," *Electr. Eng.*, vol. 103, no. 1, pp. 607–619, Feb. 2021, doi: 10.1007/s00202-020-01078-4.

[13] H. Yin, K. Zhou, and S. Yang, "Non-intrusive load monitoring by load trajectory and multi-feature based on DCNN," *IEEE Trans. Ind. Informat.*, vol. 19, no. 10 pp. 10388–10400, Oct. 2023.

[14] C. Athanasiadis, D. Doukas, T. Papadopoulos, and A. Chrysopoulos, "A scalable real-time non-intrusive load monitoring system for the estimation of household appliance power consumption," *Energies*, vol. 14, no. 3, p. 767, Feb. 2021, doi: 10.3390/en14030767.

[15] K. Hou, S. Xia, and X. Jiang, "BuMA: Non-intrusive breathing detection using microphone array," in *Proc. 1st ACM Int. Workshop Intell. Acoustic Syst. Appl.*, Jun. 2022, pp. 1–6, doi: 10.1145/3539490.3539598.

[16] B. K. Munoli, K. A. K. Jain, P. Kumar, and R. P. S. Aditya, "Human voice analysis to determine age and gender," in *Proc. Int. Conf. Recent Trends Electron. Commun. (ICRTEC)*, Feb. 2023, pp. 1–4, doi: 10.1109/ICRTEC56977.2023.10111890.

[17] M. K. Singh, S. Kumar, and D. Nandan, "Faulty voice diagnosis of automotive gearbox based on acoustic feature extraction and classification technique," *J. Eng. Res.*, vol. 11, no. 2, Jun. 2023, Art. no. 100051, doi: 10.1016/j.jer.2023.100051.

[18] J. de las Morenas, F. Moya-Fernández, and J. A. López-Gómez, "The edge application of machine learning techniques for fault diagnosis in electrical machines," *Sensors*, vol. 23, no. 5, p. 2649, Feb. 2023, doi: 10.3390/s23052649.

[19] H. Chen and S. Li, "Multi-sensor fusion by CWT-PARAFAC-IPSO-SVM for intelligent mechanical fault diagnosis," *Sensors*, vol. 22, no. 10, p. 3647, May 2022, doi: 10.3390/s22103647.

[20] Z. Cuifang, C. Yu, and M. Jiacheng, "Fabric defect detection algorithm based on PHOG and SVM," *Indian J. Fibre Textile Res.*, vol. 45, no. 1, pp. 123–126, Mar. 2020, doi: 10.56042/ijftr.v45i1.22046.

[21] B. S. Anami and M. C. Elemmi, "Comparative analysis of SVM and ANN classifiers for defective and non-defective fabric images classification," *J. Textile Inst.*, vol. 113, no. 6, pp. 1072–1082, Apr. 2022, doi: 10.1080/00405000.2021.1915559.

[22] D. L. Aguilar, M. A. Medina-Pérez, O. Loyola-González, K.-K. R. Choo, and E. Bucheli-Susarrey, "Towards an interpretable autoencoder: A decision-tree-based autoencoder and its application in anomaly detection," *IEEE Trans. Dependable Secure Comput.*, vol. 20, no. 2, pp. 1048–1059, Mar./Apr. 2023, doi: 10.1109/TDSC.2022.3148331.

[23] L. Rzayeva, A. Myrzatay, G. Abitova, A. Sarinova, K. Kulniyazova, B. Saoud, and I. Shayea, "Enhancing LAN failure predictions with decision trees and SVMs: Methodology and implementation," *Electronics*, vol. 12, no. 18, p. 3950, Sep. 2023, doi: 10.3390/electronics12183950.

[24] Z. Chen, L. Hong, Y. Gu, M. Wu, and Z. Yan, "A novel support vector machine multi-classification strategy for power transformer fault diagnosis," in *Proc. IEEE 5th Int. Electr. Energy Conf. (CIEEC)*, May 2022, pp. 3368–3373, doi: 10.1109/CIEEC54735.2022.9846531.

[25] B. Yang, J. Wang, P. Cao, T. Zhu, H. Shu, J. Chen, J. Zhang, and J. Zhu, "Classification, summarization and perspectives on state-of-charge estimation of lithium-ion batteries used in electric vehicles: A critical comprehensive survey," *J. Energy Storage*, vol. 39, Jul. 2021, Art. no. 102572, doi: 10.1016/j.est.2021.102572.

[26] Z. W. Hu and Z. H. Wang, "A non-invasive motor working state recognition method based on BP-Adaboost neural network," *Electr. Mach. Control/Dianji Yu Kongzhi Xuebao*, vol. 27, no. 10, p. 17, 2023, doi: 10.15938/j.emc.2023.10.002.

[27] Y. R. Yoon, Y. R. Lee, S. H. Kim, J. W. Kim, and H. J. Moon, "A non-intrusive data-driven model for detailed occupants' activities classification in residential buildings using environmental and energy usage data," *Energy Buildings*, vol. 256, Feb. 2022, Art. no. 111699, doi: 10.1016/j.enbuild.2021.111699.

[28] *Determination of Pilling Performance of Textile Fabrics—Part 1: Circular Trajectory Method*, GB/T Standard 4802.1-2008, 2008.

[29] *Textiles—Determination of Fabric Propensity to Surface Fuzzing and to Pilling—Part 1: Pilling Box Method*, ISO Standard 12945-1, 2020.

[30] Y. Zhang, R. Wang, S. Li, and S. Qi, "Temperature sensor denoising algorithm based on curve fitting and compound Kalman filtering," *Sensors*, vol. 20, no. 7, p. 1959, Mar. 2020, doi: 10.3390/s20071959.

[31] M. Khodarahmi and V. Maihami, "A review on Kalman filter models," *Arch. Comput. Methods Eng.*, vol. 30, no. 1, pp. 727–747, Oct. 2023, doi: 10.1007/s11831-022-09815-7.

YUANQING MAO received the master's degree in software engineering specializing in research and application development of digital technology standards from Yunnan University. Currently, he is the Deputy Director of Zhejiang Market Regulation Digital Media Center under Zhejiang Provincial Market Supervision and Administration Bureau and holding the title of a Senior Engineer, he devotes himself to the study and implementation of digital applications for market supervision and regulatory standardization.

QINGCHUN JIAO received the master's degree in information and communication engineering from Zhejiang University. Currently, he is a Professor with Zhejiang University of Science and Technology. His research endeavors concentrate on the cutting-edge domain of spatiotemporal data perception and associated intelligent analytics, with a sustained interest in the Internet of Things and the advancement of digital video intelligence processing technologies. He is dedicated to unraveling sophisticated application frameworks for spatiotemporal data intelligent analysis algorithms in challenging operational contexts. His current research endeavors are centered around security and preventive technologies, the integration of intelligent building systems, and the progressive development of smart cities, thereby contributing significantly to the realms of urban safety, efficiency, and technological innovation.

ZIFAN QIAN is currently pursuing the master's degree with the School of Automation and Electrical Engineering, Zhejiang University of Science and Technology. His research interests include image processing, deep learning, and fault diagnosis.

CHUNCONG WANG received the bachelor's degree in information management and information systems, specializing in management sciences from Ningbo Institute of Technology, Zhejiang University. Currently, she holds the position of the Deputy Director of the Second Department of Software Research and Development, Zhejiang Jinhui Digital Technology Company Ltd., and is designated as an Assistant Engineer. Her primary responsibilities involve overseeing the management of digital application projects and spearheading standardized pilot demonstration initiatives.

TINGTING SUN received the bachelor's degree from the School of Information Management and Information Technology, Zhejiang University of Finance and Economics Eastern College. Currently, she is the Deputy Director of the Textile and Leather Goods Division, Zhejiang Light Industrial Products Inspection and Research Institute, where she is engaged in work concerning textile product testing, inspection, and quality management. She is also a member of the Knitted Textile Technical Committee under the National Technical Committee for Textile Standards.